

Sulfur-alkylation-initiated Cp*Ru thiyl radicals

Richard Yee Cheong Shin ^a, Hui Shan Sim ^a, Lai Yoong Goh ^{a,*}, Richard D. Webster ^{b,*}

^a Department of Chemistry, National University of Singapore, Kent Ridge, Singapore 119260, Singapore

^b Division of Chemistry and Biological Chemistry, Nanyang Technological University, Singapore 637616, Singapore

Received 18 January 2007; received in revised form 15 March 2007; accepted 15 March 2007

Available online 21 March 2007

Abstract

The formation of thiyl radicals from [Cp*^{III}Ru{κ³SSS'-tpdt}] (**1A**) and [Cp*^{III}Ru{κ³SSN-apdt}] (**1B**) {Cp* = η⁵-C₅Me₅; tpdt = S(CH₂CH₂S⁻)₂; apdt = HN(CH₂CH₂S⁻)₂} has been initiated by thiolate alkylation or oxidation with iodine. Subsequent electron transfer processes yielded disulfide-bridged dinuclear complexes. The mechanistic pathways of these processes will be discussed.

© 2007 Elsevier B.V. All rights reserved.

Keywords: Thiyl radical; Disulfide bridge; Thiolate; Cyclopentadienyl ruthenium; Methylation

1. Introduction

The increase of interest in thiyl radicals, whether organic (*SR) or metal-bound [M(*SR)] is related to their role in biological systems [1]. The last two decades have witnessed a growing emergence of metal-thiyl radical complexes [2]. Among the early works, Sullivan and coworkers invoked the intermediacy of coordinated thiyl radicals in the conversion of a Co(III) coordinated thiolate to a Co(II) coordinated disulfide by 1-equiv. oxidants [3a]; and Treichel's group found products' evidence for the role of thiyl radicals in the oxidation of phenylthiolate-containing CpFe complexes [3b]. Stabilised thiyl complexes include RS⁺[Cr(CO)₅]₂ investigated by Darensbourg [4], a dimolybdenum species by Noble [5], a nickel species by Liaw [6], and a series of phenylthiyl-radical and related complexes of several first-row transition metals by Wieghardt [7]. Among the heavier transition metals, Ru is the only element reported to form thiyl radical species. Thus, coordinated thiyl radical intermediates were implicated in the formation of disulfide bridged Ru(II) complexes from the oxidation of

complexes of Ru(II) by Treichel [8a] and of Ru(III) by Wieghardt [8b]. Recently, Grapperhaus obtained spectroscopic, electrochemical and product evidence for Ru-coordinated thiyl radical intermediates in the oxidation reactions of [tris(phosphino)thiaphenolato]Ru(II) monoanion [2d,9].

This paper reviews our previous results on Ru-thiyl radical formation, initiated by S-alkylation of the dithiolato-thioether ligand, S(CH₂CH₂S⁻)₂, coordinated to Cp*^{III}Ru [10], and compares the results with those obtained for the analogous HN(CH₂CH₂S⁻)₂ system.

2. Results and discussion

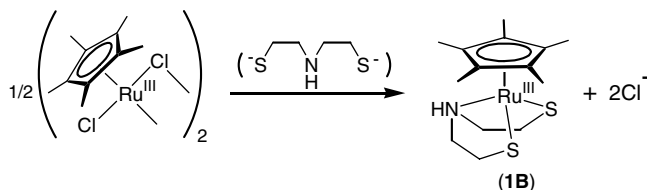
Similar to its κ³SSS'-tpdt analogue **1A** [11] {tpdt = 3-thiapentane-1,5-dithiolate, S(CH₂CH₂S⁻)₂}, complex **1B** containing κ³SSN-apdt {3-azapentane-1,5-dithiolate, HN(CH₂CH₂S⁻)₂} was obtained in high yield (81%) from the reaction of (Cp*^{III}RuCl₂)₂ with the sodium salt of the dithiolate, as shown in Scheme 1.

Methylation of **1A/1B** (notation adopted in this article for **1A** and **1B**, and other pairs of analogues) gave the disulfides **2A/2B** as the major product together with the dimethylated species **3A/3B** (Scheme 2).

The formation of these products could be rationalized based on an initial electrophilic attack of Me⁺ on a

* Corresponding authors. Tel.: +65 67791691; fax: +65 67911961.

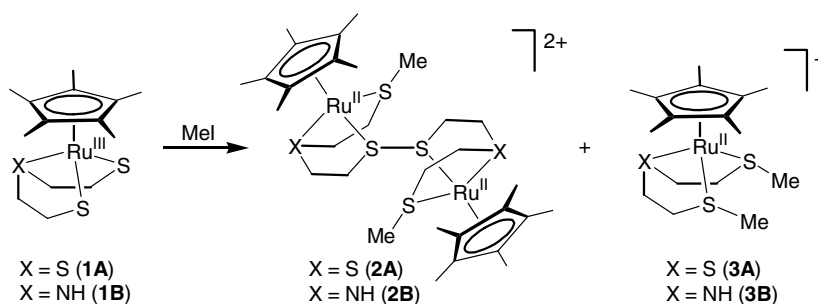
E-mail addresses: chmgohly@nus.edu.sg (L.Y. Goh), webster@ntu.edu.sg (R.D. Webster).

Scheme 1. Synthesis of **1B**.

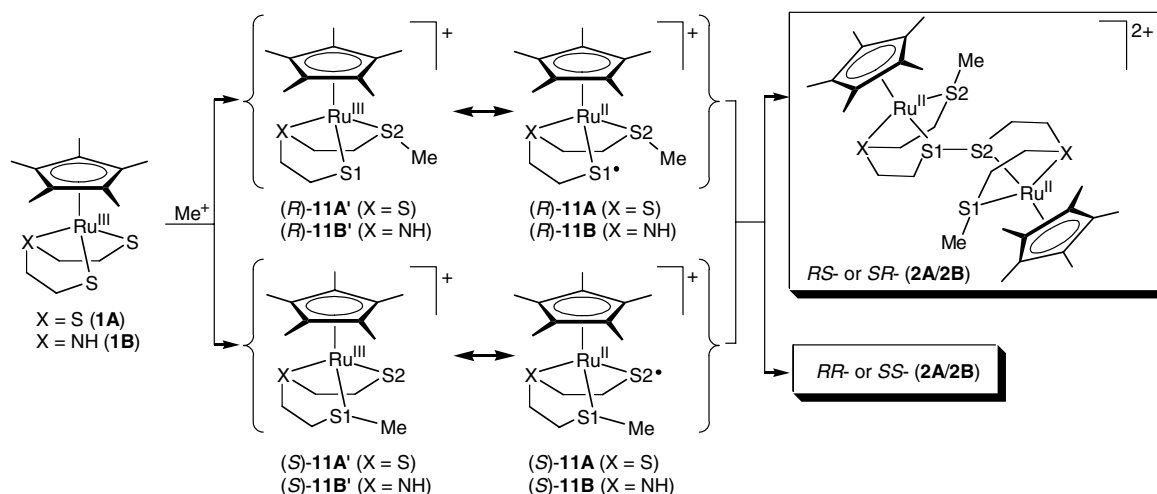
thiolate sulfur of **1A/1B**, thus generating racemic Ru(III) intermediates (*R*)-**11A'**/**11B'** and (*S*)-**11A'**/**11B'**. An *internal electron transfer* (IET) in the *R* or *S* intermediates then leads to the respective cationic Ru(II) sulfur-centered radicals (*R*)-**11A/11B** and (*S*)-**11A/11B**; coupling of these thiyl radicals would give two pairs of S–S bonded dinuclear diastereomers, viz. the *RS*, *SR* pair and the *RR*, *SS* pair (Scheme 3), detectable in the variable temperature proton NMR spectrum of **2A**. However, only the *RS* and *SR* enantiomeric pair had been crystallized out and hence characterized crystallographically. Such metal thiyl radicals, formed via oxidation of metal thiolates, had been invoked as intermediates in the formation of coordinated disulfides by Sullivan [3a], of a tris-disulfide bridged diruthenium complex by Wiegardt [8b], and in carbon–sulfur bond formation with methyl ketones by Grapperhaus [9].

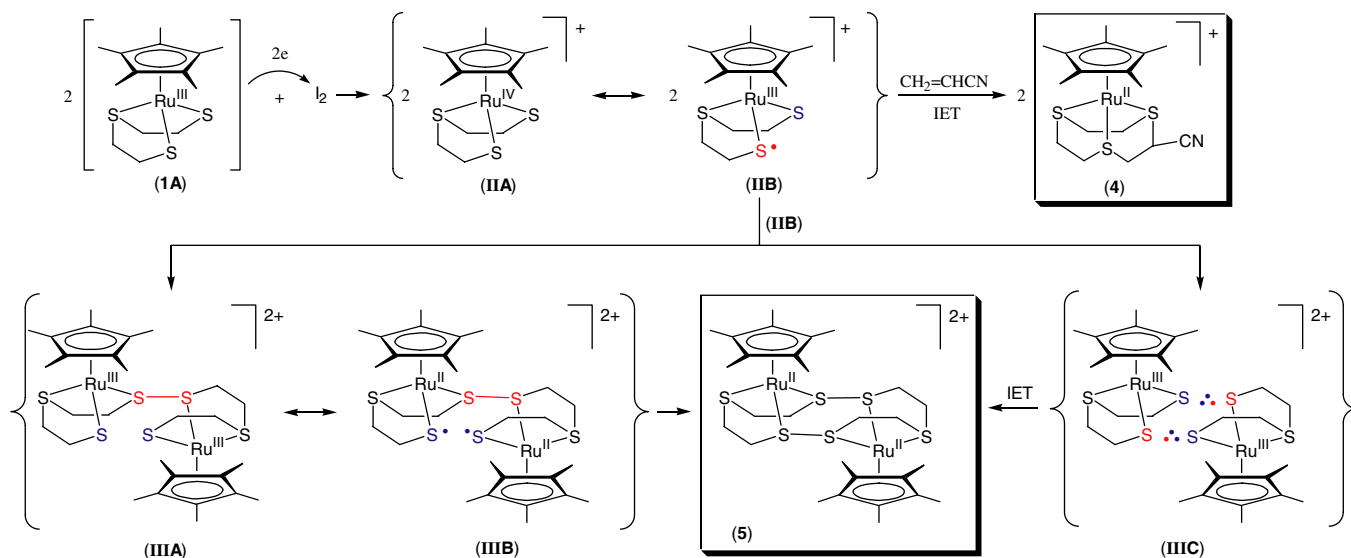
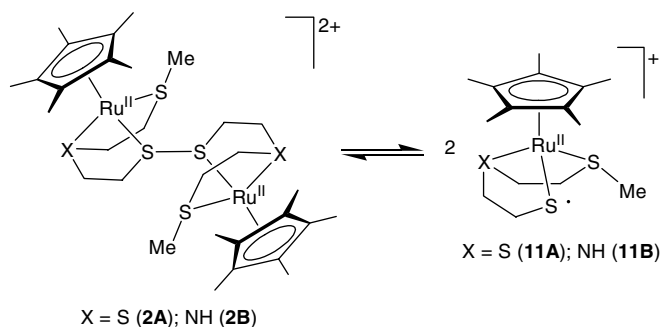
The radical nature of this reaction was established via reactions of **1A** with methylating reagents in the presence of acrylonitrile (AN), a strongly electrophilic alkene known to react readily with thiyl and other non-carbon radicals [12]. It was found that in the presence of a 10-fold excess of AN, a Ru(II) AN adduct **4**, containing a $\kappa^3SS'S''$ -cyano-substituted 9S3 ligand, was an additional product in substantial proportion, while the relative yield of the disulfide **2A** varied with solvent and the nature of the alkylating agent, on account of its subsequent facile reaction with **1A** (discussed below).

Complex **4** was the sole product from the reaction of **1A** with I_2 in the presence of AN. In the absence of AN, the instantaneous reaction of **1A** with I_2 led to the isolation of complex **5**, in high yield (Scheme 4). Based on electrochemical evidence, the transformations are envisaged to go via a Ru(IV) species **IIA**, which underwent intramolecular electron rearrangement to generate a Ru(III) S-centered radical **IIIB**. In the presence of AN, the S-centered radical **IIIB** was effectively trapped to form the AN adduct **4**. We note that Grapperhaus lately reported a similar carbon–sulfur bond formation between a Ru(III) thiyl radical and the enol tautomer of acetone [9]. In the absence of AN, **IIIB** dimerizes to form **IIIA**. A repeat intramolecular electron arrangement then gives the Ru(II)–Ru(II) di-radical

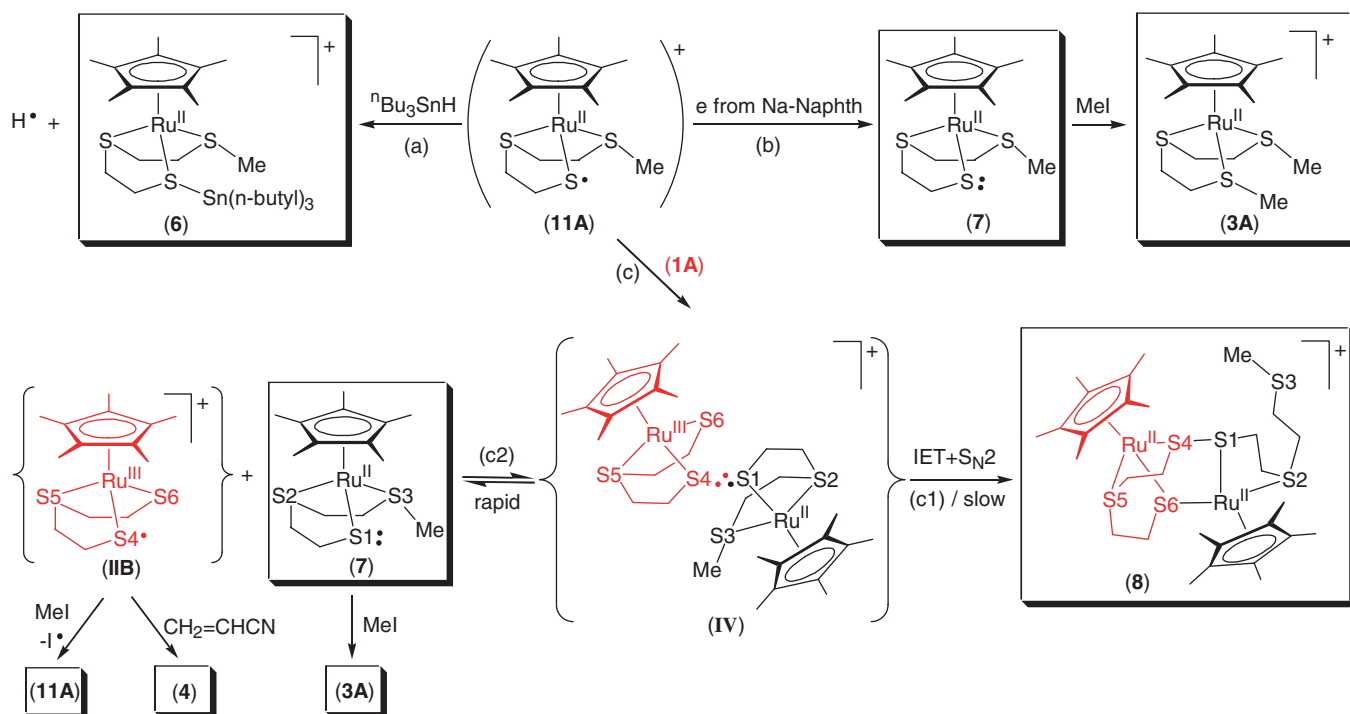


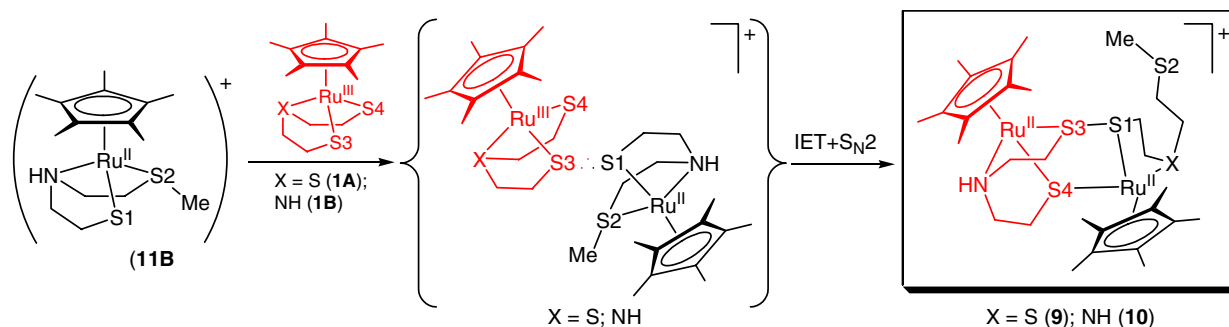
Scheme 2. Methylation reactions.

Scheme 3. Mechanistic pathway for the formation of **2A** and **2B**.

Scheme 4. Redox interaction between **1A** and I_2 .Scheme 5. Reversible dissociation of **2A** and **2B** in solution.

1IB, which undergoes a second S–S coupling to give species **5**, containing a centrosymmetric Ru_2S_4 core with the two Ru centers in a *trans* configuration. Alternatively, twice coupling of the S radical of **1IB** with a lone pair on the thiolate S of a second unit of the same moiety would generate simultaneously two $2c/3e$ S–S bonds forming species **1IIIC**. Such $(\sigma)^2(\sigma^*)^1$ odd-electron bonds are a common type of bond in heteroatom-centered radicals and radical ions [13]. The higher-energy electron in the σ^* orbital of this bond would readily be transferred to the Ru centers giving the Ru(II)–Ru(II) species **5**.

Scheme 6. Reactions of **11A**.

Scheme 7. Reaction of **11B** with **1A** and **1B**.

The interaction of **2A** with **1A** arises from the facile reversible dissociation of **2A** into the mononuclear cation radical **11A** (Scheme 5). This dissociation is supported by evidence from a combination of electrochemical, EPR, UV–Vis and NMR experiments. Various aspects of the reactivity features of **11A** have been reported previously [10] and are summarized in Scheme 6. Thus, it reacted as a radical initiator with Bu_3SnH , abstracting the radical $\text{Bu}_3\text{Sn}^\cdot$ to form the RuSSnBu_3 -containing complex **6** (route (a)). In the reaction with sodium naphthalide (route (b)), an electron reduces **11A**, generating complex **7**, which was isolated and readily alkylated to give **3A**. The interaction of **11A** with **1A** (route (c)) had led to isolation of the dinuclear species **8**. It was proposed that the formation of **8** involves the formation of an intermediate **IV** via coupling of the S-centered radical in **11A** and the S lone pair of **1A** to give a $\text{S1}:\text{S4}$ (2c/3e) disulfide bond. As in **IIIc** (Scheme 4), the transfer of the σ^* electron in this bond to Ru(III) resulted in a Ru(II) center and the S1–S4 bond formation. Finally, complex **8** would result from a concomitant or subsequent intramolecular nucleophilic attack of thiolate S6 on the other Ru(II) center, leading to displacement of the ligated S3Me moiety, thus generating the $(\text{CH}_2)_2\text{S3Me}$ pendant chain at S2 (route (c1)). Simultaneously, the weak $\text{S1}:\text{S4}$ bond in **IV** could undergo reversible cleavage to the S4-centered radical **11B** and species **7** containing a lone pair electron at S1 (route (c2)); in essence this constitutes an inner-sphere transfer of an electron from **1A** to **11A**. The interaction of **11B** and **7** with AN and MeI, respectively, then gave the isolated species **4** and **3A**. In the presence of MeI alone, it is highly likely that **11B** would be converted via a radical pathway to species **11A**, which on dimerization would regenerate **2A**.

While the reaction of **11A** with **1A** yielded **8**, the analogous reaction of **11B** with **1A/1B** gave **9** and **10** (Scheme 7), respectively, following a similar pathway described in Scheme 6 (route c and c1).

2.1. Electrochemical studies

Cyclic voltammograms of **1B** and **2B** in CH_2Cl_2 at 293 and 233 K are shown in Fig. 1. **1B** was observed to undergo an oxidation process at relatively negative potentials

(-0.75 V vs. Fc/Fc^+). The anodic (E_p^{ox}) to cathodic (E_p^{red}) peak-to-peak separation ($\Delta E_{\text{pp}} = 78$ mV) was similar to that observed for ferrocene under identical conditions suggesting that the process occurs *via* one-electron. The anodic (i_p^{ox}) to cathodic (i_p^{red}) peak current ratio remained equal to unity at 293 and 233 K indicating that the process involved a chemically reversible oxidation with the oxidised compound (**1B** $^+$) stable for at least a few seconds.

2B displayed one oxidation process at $+0.235$ V and one reduction process at -0.935 V vs. Fc/Fc^+ , although close examination of the voltammetric behaviour indicated that the redox chemistry was complex. The peak currents measured during the oxidation and reduction of **2B** were approximately twice that measured for the oxidation of

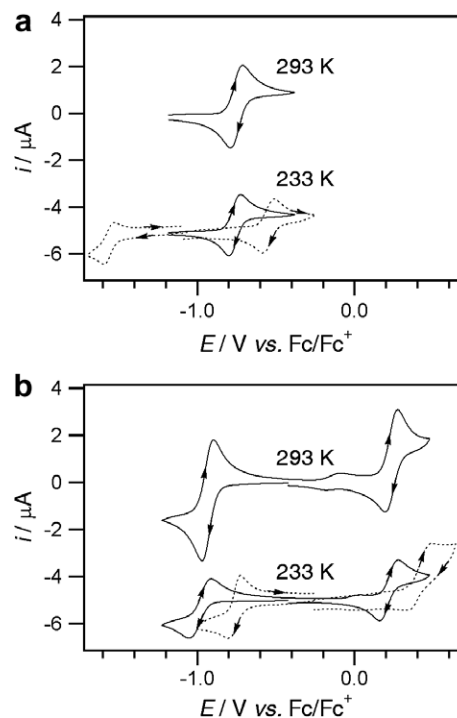


Fig. 1. Cyclic voltammograms of 1.0 mM analytes recorded at a scan rate of 100 mV s^{-1} in CH_2Cl_2 solutions containing 0.25 M Bu_4NPF_6 at 1 mm diameter planar electrodes. (a) (—) **1B**, (⋯) **1A**. (b) (—) **2B** (dissociates into 2 mol of **11B**), (⋯) **11A**. Voltammograms recorded at 233 K are offset by $-5 \mu\text{A}$. **1B** and **11B** were measured on Pt, while **1A** and **11A** were measured on GC with the data taken from Ref. [10].

Table 1

Cyclic voltammetric data obtained for 1 mM analytes in CH₂Cl₂ solutions at a scan rate of 100 mV s⁻¹ at 1 mm diameter Pt or GC electrodes at 293 K or 233 K with 0.25 M Bu₄NPF₆ as the supporting electrolyte

Compound	Voltammetric processes ^a							
	Reduction				Oxidation			
	$E_p^{\text{red}}/\text{V}^c$	$E_p^{\text{ox}}/\text{V}^b$	$E_{1/2}^{\text{r}}/\text{V}^d$	$\Delta E/\text{mV}^e$	$E_p^{\text{ox}}/\text{V}^b$	$E_p^{\text{red}}/\text{V}^c$	$E_{1/2}^{\text{r}}/\text{V}^d$	$\Delta E/\text{mV}^e$
1B	ND	ND	ND	ND	-0.713	-0.791	-0.750	78
1A	-1.596	-1.528	-1.560	68	-0.512	-0.586	-0.550	74
2B/11B	-0.973	-0.899	-0.935	74	+0.273	+0.193	+0.235	80
2A/11A	-0.806	-0.726	-0.765	80	+0.488	ND	ND	ND

ND, not determined. **1B** and **2B/11B** were measured with a Pt electrode at 293 K, while **1A** and **2A/11A** were measured with a GC electrode at 233 K with the data taken from Ref. [10].

^a All potentials are relative to the ferrocene/ferrocenium redox couple.

^b E_p^{ox} = oxidative peak potential.

^c E_p^{red} = reductive peak potential.

^d $E_{1/2}^{\text{r}} = (E_p^{\text{ox}} + E_p^{\text{red}})/2$ (measured to nearest 5 mV).

^e $\Delta E = |E_p^{\text{ox}} - E_p^{\text{red}}|$.

equivalent concentrations of **1B** (compare Fig. 1a and b). Considering that **2B** is dimeric, the difference in peak current peak between **1B** and **2B** can be rationalised by **2B** undergoing a *two*-electron oxidation and *two*-electron reduction. In order for this to occur, it is necessary for the two redox centres in **2B** to be non-communicating, so that one-electron is added/removed to/from each half of the molecule simultaneously (two electrons overall).

An alternative mechanism to account for the electrochemistry of **2B** is available based on the results of a previous study on compounds **1A**, **2A** and **7** [10]. It was established that in solution, the closely related compound **2A** undergoes a monomerization reaction to form 2 mols of **11A** (Scheme 5), so that cyclic voltammograms performed on solid samples of **2A** dissolved in CH₂Cl₂, show only the presence of **11A** [10]. The dashed lines in Fig. 1 show voltammograms of **1A** and **11A** performed under the same conditions as **1B** and **2B**, which appear very similar except that they are shifted to more positive potentials by ~0.2 V (due to the presence of the amine linkage in **1B** and **11B**). Therefore, it is likely that the solution phase

behaviour of **2B** is the same as that of **2A**, with the voltammetry shown in Fig. 1b attributable to the monomeric compound **11B**.

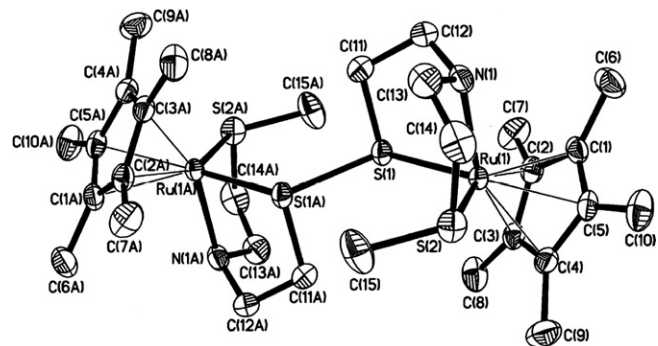


Fig. 3. ORTEP plot for **2B** dication (50% probability thermal ellipsoids, hydrogen atoms omitted).

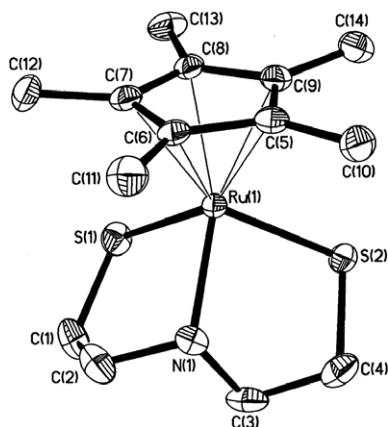


Fig. 2. ORTEP plot for **1B** (50% probability thermal ellipsoids, hydrogen atoms omitted).

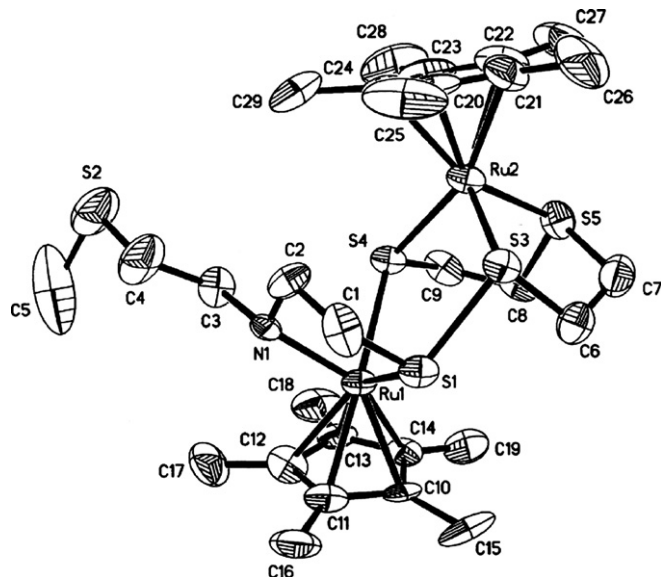


Fig. 4. ORTEP plot for **9** monocation (50% probability thermal ellipsoids, hydrogen atoms omitted).

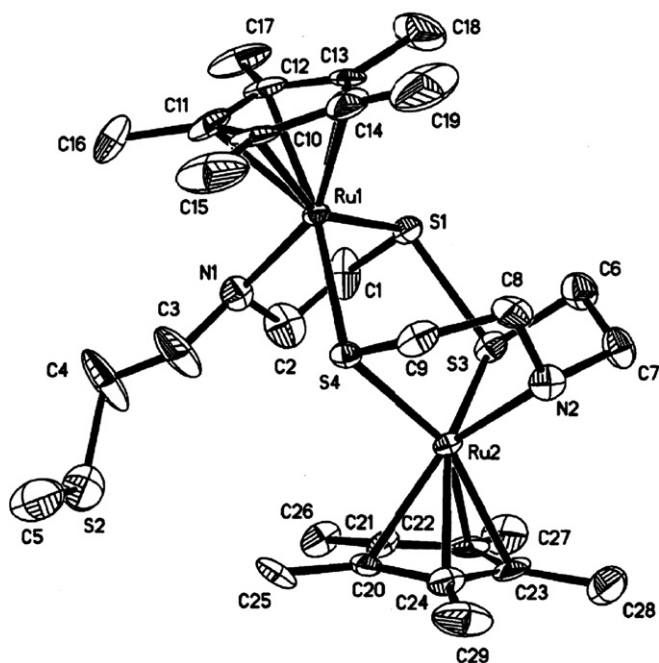


Fig. 5. ORTEP plot for **10** monocation (50% probability thermal ellipsoids, hydrogen atoms omitted).

The conclusion that the voltammetry in Fig. 1 is from solutions of **11B** (rather than **2B**) is supported by the low temperature experiments (233 K) that show a large decrease in peak currents compared to the higher temperature (293 K) experiments. While there is expected to be a decrease in peak current at low temperatures due to decreasing diffusion coefficients, the relative decrease in current is much larger than that observed for **1B** when going from 293 to 233 K. EPR experiments previously demonstrated that the equilibrium between **2A** and **11A** shifts towards the dimer (**2A**) at low temperatures, therefore, the reason for the larger than expected decrease in current as the temperature is lowered in Fig. 1b, is likely

to be caused by a decrease in concentration of **11B** to form **2B** (in addition to a diminishing diffusion coefficient value) (see Table 1).

2.2. Structural analyses

The ORTEP diagrams of the monomeric, neutral complex $[\text{Cp}^*\text{Ru}(\kappa^3\text{SSN}-\text{C}_4\text{H}_9\text{S}_2\text{N})]$ (**1B**), and of the disulfide diruthenium complexes **2B**, **9**, and **10** are shown in Figs. 2–5, respectively. Selected bond distances and angles for the complexes are listed in Table 2. In complex **1B** the ruthenium atom is surrounded in the usual piano-stool arrangement by the planar $\eta^5\text{-Cp}^*$ ring together with two thiolate sulfur atoms and one amine nitrogen atom of the ‘apdt’ dianion. In comparison to **1A** [11], it is noted that the replacement of a S atom by a (smaller) N atom in the ligand has resulted in larger S–Ru–S angles ($108.83(5)^\circ$ in **1B** vs. $92.18(4)^\circ$ in **1A**), and shorter Ru–S(thiolate) bond lengths ($2.3150(12)$ Å, av in **1B** vs. $2.3829(12)$ Å (av.) in **1A**).

$(\text{Cp}^*\text{Ru})_2$ ($\mu\text{-S}_2$) complexes. The molecular structure of the disulfide diruthenium complex **2B** possesses a center of inversion at the mid-point of the S–S bond, which bridges two Cp^*Ru units in a *trans* $\eta^1\text{-}\eta^1$ configuration. As in the **2A** analogue, the structure belongs to the *RS* or *SR* diastereomer. The disulfide bond in **2B** ($2.2304(15)$ Å) is slightly longer than that in **2A** ($2.194(3)$ Å).

The molecular structures of the analogues **9** and **10** are very similar (Figs. 3 and 4). Each contains two Cp^*Ru moieties linked by a *cis* $\mu\text{-}\eta^1\text{-}\eta^1$ S(1)–S(3) bridge and a μ -thiolate moiety (S(4)), and an ‘alkylated’ pendant $\text{CH}_2\text{-CH}_2\text{S(2)Me}$ side arm which was generated by an intramolecular nucleophilic attack of thiolate S4 onto the Ru(1) atom, displacing the S2 donor atom. The S–S distances of **2B**, **9**, and **10** (range $2.2304(15)$ – $2.342(4)$ Å) are close to values reported by Wieghardt for the tris *cis* $\eta^1\text{-}\eta^1\text{-S}_2$ bridged Ru(II)SSRu(II) complex ($2.198(1)$ – $2.2152(7)$ Å) [8b]; these distances are longer than the normal single bond

Table 2
Selected bond lengths (Å) and angles ($^\circ$) of the ‘apdt’ complexes

1B		2B ^a		9		10	
Ru(1)–S(1)	2.3153(12)	Ru(1)–S(1) ^b	2.2756(8)	Ru(1)–S(1) ^b	2.244(4)	Ru(1)–S(1) ^b	2.238(3)
Ru(1)–S(2)	2.3146(12)	Ru(1)–S(2)	2.3438(9)	Ru(1)–S(4)	2.464(4)	Ru(1)–S(4)	2.432(3)
Ru(1)–N(1)	2.140(4)	Ru(1)–N(1)	2.165(3)	Ru(1)–N(1)	2.191(12)	Ru(1)–N(1)	2.213(11)
		S(1)–S(1A)	2.2304(15)	Ru(2)–S(3) ^b	2.241(4)	Ru(2)–S(3) ^b	2.236(3)
				Ru(2)–S(4)	2.412(4)	Ru(2)–S(4)	2.396(3)
				Ru(2)–S(5)	2.296(4)	Ru(2)–N(2)	2.166(10)
				S(1)–S(3)	2.312(6)	S(1)–S(3)	2.342(4)
S(1)–Ru(1)–S(2)	108.83(5)	S(1)–Ru(1)–S(2)	108.69(3)	S(1)–Ru(1)–S(4)	94.26(14)	S(1)–Ru(1)–S(4)	97.07(11)
S(1)–Ru(1)–N(1)	81.24(11)	S(1)–Ru(1)–N(1)	82.84(8)	S(1)–Ru(1)–N(1)	83.6(3)	S(1)–Ru(1)–N(1)	83.9(3)
S(2)–Ru(1)–N(1)	82.45(11)	S(2)–Ru(1)–N(1)	82.92(8)	S(4)–Ru(1)–N(1)	83.1(3)	S(4)–Ru(1)–N(1)	83.9(3)
		Ru(1)–S(1)–S(1A)	123.71(5)	S(3)–Ru(2)–S(4)	95.07(14)	S(3)–Ru(2)–S(4)	98.12(11)
				S(3)–Ru(2)–S(5)	87.98(16)	S(3)–Ru(2)–N(2)	83.0(3)
				S(4)–Ru(2)–S(5)	86.41(15)	S(4)–Ru(2)–N(2)	83.5(3)
				Ru(1)–S(4)–Ru(2)	118.92(15)	Ru(1)–S(4)–Ru(2)	117.06(12)

^a The molecule possesses a center of inversion.

^b Pertaining to the RuSSRu moiety.

(cf. S–S single bond = 2.04–2.10 Å in S₈ [14] and 2.038 Å in dimethyl disulfanes [15]). Specifically they are longer than those found in the ‘inorganic’ (μ-S₂) cores of Ru₂(III,III) complexes found in the literature (range 1.962(4)–2.014(1) Å) [16–18], as well as in the (μ-SR₂) cores of Matsumoto’s Ru₂(III,III) complexes (range 2.093(5)–2.164(5) Å) [19]. The elongation of the S–S bond in these Ru₂ cores are in agreement with the π-MO description of the RuS–SRu core, in which the two unpaired electrons of the two Ru(III) atoms occupy a distinct antibonding π-MO as an electron pair, resulting in a decrease of bond order [18,20,21].

3. Conclusion

The methylation of a *cis*-dithiolate ligand at Ru(III) has resulted in mono-sulfur alkylation and initiated an electron transfer process, which produced a Ru-thiyl radical with subsequent coupling to a disulfide bridged species. The facile homolytic dissociation of this disulfide bond generated a rich radical-based S-centered reactivity. Iodine oxidation of the Cp*Ru(III) dithiolate under investigation also produced thiyl radicals which resulted in a double-disulfide bridged dinuclear species. In context, we note that a similar oxidation of [Ru(III)L], where L is a κ³N-1,4,7-triazacyclononane species, had produced a tris-disulfide bridged Ru₂ compound [8b]. The alkylation-initiated thiyl radical formation found in this study appears to be a unique feature of the Cp*Ru(III) moiety, observed here with two dithiolato ligands, viz. κ³SSS'-tpdt and κ³SSN-apdt. Indeed, there is no evidence of any such occurrence in a related (hexamethylbenzene)Ru(II) complexes [22], nor has it been observed before in alkylation of *cis*-dithiolate ligands at Ni(II) [23], Mo(0) [24] or Co(II) and Rh(III) [25]. It is conceivable that the internal electron transfers postulated in the observed transformations of these Ru(III) complexes are facilitated by the relatively higher stability of d⁶-Ru(II) vs. Ru(III) or Ru(IV) oxidation states.

4. Experimental

4.1. General procedures

All general procedures were as previously described [11]. [Cp*RuCl₂]₂ was synthesised from RuCl₃ · nH₂O (Oxkem) as described in the literature [26]. HN(CH₂CH₂SH)₂ was prepared as previously reported [27]. Voltammetric experiments were conducted with a computer controlled Eco Chemie μAutolab III potentiostat with 1 mm diameter planar Pt or GC working electrodes, an Ag wire reference electrode separated from the test solution with a salt bridge containing 0.5 M Bu₄PF₆ in CH₃CN, and a Pt wire auxiliary electrode. Potentials were referenced to the ferrocene/ferrocenium (Fc/Fc⁺) redox couple, which was used as an external standard. The electrochemical cell was thermostated at 233 and 293 K using an Eyela PSL-1000 variable temperature cooling bath.

4.2. Synthesis of **1B**

Bis(2-mercaptoethyl)amine (0.195 mL, 1.56 mmol) was injected into a suspension of sodium methoxide (freshly generated from sodium (66.5 mg, 2.89 mmol) in MeOH) in THF (15 mL), and the mixture allowed to stir overnight at ambient temperature. [(Cp*RuCl₂)₂] (0.277 g, 0.451 mmol) was then added as a solid to the viscous suspension, which turned purple instantaneously. After stirring for 3 h at ambient temperature, the mixture was filtered through a disc of alumina (3 × 1 cm²) to remove the fine white solids of NaCl. The purple filtrate was evacuated to dryness and the residue recrystallised in acetonitrile–ether. Dark purple crystals of [Cp*Ru(C₄H₉S₂N)] (**1B**) (0.203 g, 0.546 mmol, 60% yield) were collected after 14 h at –30 °C, followed by subsequent crops (total 0.069 g, 0.186 mmol, 21% yield). Diffraction-quality crystals were selected from the crops of crystals obtained above. No signals were observed in the ¹H NMR spectrum in CD₃CN at room temperature. FAB⁺ MS: *m/z* 372 [M]⁺. IR (ν cm⁻¹, KBr): 3104 m (N–H), 2969 wsh, 2949 m, 2905 m, 2846 m, 2800 wsh, 1483 wsh, 1440 m, 1373 m, 1360 w, 1344 w, 1287 w, 1263 w, 1231 w, 1217, 1188 w, 1154 vw, 1131 wsh, 1086 m, 1071 m, 1017 m, 997 m, 967 m, 917 w, 845 w, 799 m, 670 w, 608 vw, 586 vw, 536 vw. Anal. Calc. (Found) for **1B** (C₁₄H₂₄NS₂Ru): C, 45.3 (45.4); H, 6.5 (6.5); N, 3.8 (4.4); S, 17.3 (16.2)%.

4.3. Reaction of **1B** with MeI – synthesis of **2B**

To a dark purple solution of **1B** (35 mg, 0.09 mmol) in MeOH (15 mL) was added MeI (35 μL, 0.56 mmol) with stirring. A color change to dark red was observed immediately. After stirring for 4 h, the reaction mixture was evacuated to dryness to remove the excess MeI. The red residue was redissolved in MeOH (8 mL) and NH₄PF₆ (60 mg, 0.37 mmol) added with stirring. The precipitated dark red solids were filtered and the solids extracted with CH₃CN (2 × 5 mL) giving a dark red solution, which upon concentration and addition of ether gave fine red microcrystals of [{Cp*Ru}₂{S(CH₂)₂NH(CH₂)₂SMe}₂](PF₆)₂ (**2B**) (37 mg, 74% isolated yield) after 24 h at –30 °C. The mass spectrum of the mother liquor shows the presence of **3B** at *m/z* 402. Diffraction-quality crystals of **2B** were obtained by diffusion of ether into an acetonitrile solution for 2 weeks at –30 °C. No signals were observed in the ¹H NMR spectrum in CD₃CN at room temperature. FAB⁺ MS: *m/z* 919 [M – PF₆]⁺, 387 [M – 2PF₆]²⁺. FAB⁻ MS: *m/z* 145 [PF₆]⁻. IR (ν cm⁻¹, KBr): 3292 m (N–H), 2957 wsh, 2919 m, 2867 wsh, 1451 m, 1411 m, 1383 m, 1068 m, 1025 m, 959 m, 919 w, 840 vs (PF₆), 788 m, 740 w, 557 s (PF₆). Anal. Calc. (Found) for **2B** (C₃₀H₅₄F₁₂N₂P₂Ru₂S₄): C, 33.9 (34.1); H, 5.1 (4.8); N, 2.6 (2.8); S, 12.1 (12.1)%.

4.4. Reaction of **1A** with **2B** – synthesis of **9**

To a stirred dark red solution of **2B** (15 mg, 0.01 mmol) in CH₃CN (10 mL) was added solid **1A** (11 mg,

0.03 mmol). The color changed from purple to brown after 20 min, but the mixture was left stirring for 5 h. It was then evacuated to dryness. The blackish oily residue was triturated with toluene (3 × 3 mL) to extract the slight excess of **1A** used. The residual solids were then recrystallized in CH₂Cl₂/ether to give dark red orthorhombic crystals of [$\{\text{Cp}^*\text{Ru}\}_2\{\text{MeS}(\text{CH}_2)_2\text{NH}(\text{CH}_2)_2\text{SS}(\text{CH}_2)_2\text{S}(\text{CH}_2)_2\text{S}\}$]PF₆, **9** (22 mg, 54% yield) after 1 day at –30 °C. ¹H NMR (300 MHz, δ, CD₃CN): 3.52–3.46 (8-line m, 1H, SCH₂), 2.92–2.81 (6-line m, 4H, SCH₂), 2.71–2.62 (m, 2H, SCH₂), 2.57–2.47 (8-line m, 3H, SCH₂), 2.41–2.28 (10-line m, 2H, SCH₂), 2.09 (s, 3H, SMe), 1.73 (s, 15H, C₅Me₅), 1.67 (s, 15H, C₅Me₅), 1.54–1.43 (6-line m, 1H, SCH₂), 0.39–0.29 (6-line m, 1H, SCH₂), 0.21–0.02 (13-line m, 2H, SCH₂). ¹³C NMR (300 MHz, δ, CD₃CN): 93.7, 88.4 (C₅Me₅), 54.2, 46.3, 43.4, 36.7, 36.2, 35.5, 35.1, 32.4 (SCH₂), 15.8 (SMe), 10.5, 10.3 (C₅Me₅). FAB⁺ MS: *m/z* 776 [M–PF₆]⁺. FAB[–] MS: *m/z* 145 [PF₆][–]. IR (ν cm^{–1},

KBr): 3283 w (N–H), 2964 wsh, 2907 m, 1455 m, 1410 m, 1381 m, 1261 w, 1154 w, 1066 w, 1026 m, 964 w, 917 w, 843 vs (PF₆), 737 w, 558 s (PF₆). Anal. Calc. (found) for **9** (C₂₉H₅₀F₆NPRu₂S₅ · 1/2CH₂Cl₂): C, 36.8 (36.9); H, 5.3 (5.1); N, 1.5 (1.5); S, 16.7 (17.4)%.

4.5. Reaction of **1B** with **2B** – synthesis of **10**

To a stirred dark red solution of **2B** (18 mg, 0.02 mmol) in CH₃CN (10 mL) was added solid **1B** (13 mg, 0.03 mmol). The color gradually changed from reddish to dark brown. After stirring for 3 h, the solution was filtered from some blackish solids and the filtrate evacuated to dryness. The dark brown residue was recrystallized in CH₂Cl₂/ether to give black crystals of [$\{\text{Cp}^*\text{Ru}\}_2\{\text{MeS}(\text{CH}_2)_2\text{NH}(\text{CH}_2)_2\text{SS}(\text{CH}_2)_2\text{NH}(\text{CH}_2)_2\text{S}\}$]PF₆, **10** (22 mg, 70% yield) after 1 day at –30 °C. ¹H NMR (400 MHz, δ, CD₃CN): 3.57 (br s, 2H, NH), 3.31–3.27 (4-line m, 1H,

Table 3
Data collection and processing parameters

Complexes	1B	2B	9	10
Formula	C ₁₄ H ₂₄ NRuS ₂	C ₃₄ H ₆₀ F ₁₂ N ₄ P ₂ Ru ₂ S ₄	C ₃₁ H ₅₄ Cl ₄ F ₆ NPRu ₂ S ₅	C ₂₉ H ₅₁ F ₆ N ₂ PRu ₂ S ₄
<i>M_r</i>	371.53	1145.18	1089.96	903.07
Temperature (K)	223(2)	223(2)	223(2)	223(2)
Crystal color and habit	Dark purple, needle	Dark red, orthorhombic	Dark brown, orthorhombic	Black, orthorhombic
Crystal size (mm)	0.30 × 0.10 × 0.04	0.04 × 0.12 × 0.20	0.24 × 0.20 × 0.04	0.16 × 0.08 × 0.06
Crystal system	Orthorhombic	Triclinic	Triclinic	Monoclinic
Space group	<i>Pbca</i>	<i>P</i> $\bar{1}$	<i>P</i> $\bar{1}$	<i>P2</i> (1)/ <i>c</i>
<i>a</i> (Å)	9.9108(6)	10.2936(5)	11.692(7)	12.1648(9)
<i>b</i> (Å)	16.7046(10)	11.5407(6)	13.434(8)	18.7979(15)
<i>c</i> (Å)	18.7762(11)	12.1641(6)	15.894(9)	15.6434(11)
α (°)	90	63.234(1)	75.722(8)	90
β (°)	90	65.700(1)	73.322(7)	93.202(2)
γ (°)	90	67.340(1)	66.120(7)	90
<i>V</i> (Å ³)	3108.5(3)	1138.75(10)	2162(2)	3571.6(5)
<i>Z</i>	8	1	2	4
Density (g cm ^{–3})	1.588	1.670	1.674	1.679
Absorption coefficient (mm ^{–1})	1.261	0.997	1.275	1.179
<i>F</i> (000)	1528	582	1104	1840
θ Range for data collection	2.17–27.49	1.96–27.50	1.68–22.50	1.68–25.00
Index ranges	–12 ≤ <i>h</i> ≤ 12, –14 ≤ <i>k</i> ≤ 21, –24 ≤ <i>l</i> ≤ 24	–13 ≤ <i>h</i> ≤ 13, –14 ≤ <i>k</i> ≤ 14, –15 ≤ <i>l</i> ≤ 15	–12 ≤ <i>h</i> ≤ 12, –14 ≤ <i>k</i> ≤ 14, –17 ≤ <i>l</i> ≤ 17	–14 ≤ <i>h</i> ≤ 7, –22 ≤ <i>k</i> ≤ 22, –18 ≤ <i>l</i> ≤ 18
Number of reflections collected	20,632	14,978	14,890	20,494
Independent reflections	3569	5222	5660	6292
Maximum and minimum transmission	0.9513 and 0.7035	0.9612 and 0.8255	0.9508 and 0.7496	0.9326 and 0.8337
Number of data/restraints/parameters	3569/0/259	5222/0/273	5660/64/478	6292/150/414
Final <i>R</i> indices [<i>I</i> > 2σ(<i>I</i>)] ^{a,b}	<i>R</i> ₁ = 0.0556, <i>wR</i> ₂ = 0.1049	<i>R</i> ₁ = 0.0417, <i>wR</i> ₂ = 0.0970	<i>R</i> ₁ = 0.0931, <i>wR</i> ₂ = 0.2083	<i>R</i> ₁ = 0.0986, <i>wR</i> ₂ = 0.1972
<i>R</i> indices (all data)	<i>R</i> ₁ = 0.0701, <i>wR</i> ₂ = 0.1101	<i>R</i> ₁ = 0.0471, <i>wR</i> ₂ = 0.0998	<i>R</i> ₁ = 0.1483, <i>wR</i> ₂ = 0.2309	<i>R</i> ₁ = 0.1347, <i>wR</i> ₂ = 0.2138
Goodness-of-fit on <i>F</i> ^{2c}	1.217	1.091	1.063	1.137
Large difference in peak and hole (e Å ^{–3})	0.979 and –1.636	0.957 and –0.603	1.550 and –1.082	1.628 and –1.528

^a $R = (\sum |F_o| - |F_c|) / \sum |F_o|$.

^b $wR_2 = [(\sum \omega |F_o| - |F_c|)^2 / \sum \omega |F_o|^2]^{1/2}$.

^c Goodness-of-fit = $[(\sum \omega |F_o| - |F_c|)^2 / (N_{\text{obs}} - N_{\text{param}})]^{1/2}$.

SCH₂), 2.94–2.89 (4-line m, 1H, SCH₂), 2.81–2.56 (m, 3H, SCH₂), 2.51–2.35 (m, 4H, SCH₂), 2.30–2.22 (m, 4H, SCH₂), 2.09 (s, 3H, SMe), 1.69 (s, 15H, C₅Me₅), 1.68 (s, 15H, C₅Me₅), 1.02–0.95 (6-line m, 1H, SCH₂), 0.12–0.02 (9-line m, 1H, SCH₂), –0.12–0.22 (10-line m, 1H, SCH₂). ¹³C NMR (400 MHz, δ, CD₃CN): signal very weak (C₅Me₅), 60.8, 48.9, 42.4 (SCH₂), 11.3 (SMe), signal very weak (C₅Me₅). FAB⁺ MS: *m/z* 759 [M–PF₆]⁺. FAB[–] MS: *m/z* 145 [PF₆][–]. IR (ν cm^{–1}, KBr): 3303 w (N–H), 2964 wsh, 2911 m, 2857 wsh, 1412 m, 1381 m, 1285 vw, 1260 w, 1192 vw, 1067 w, 1027 m, 953 w, 921 vw, 841 vs (PF₆), 739 vw, 558 s (PF₆). Anal. Calc. (found) for **10** (C₂₉H₅₁N₂F₆PRu₂S₄): C, 38.6 (38.4); H, 5.7 (5.8); N, 3.1 (3.5); S, 14.2 (14.2)%.

4.6. X-ray crystal structure determinations

The crystals were mounted on glass fibers. X-ray data were collected on a Bruker AXS SMART APEX CCD diffractometer, using Mo Kα radiation (λ = 0.71073 Å) at 223 K. The program SMART [28] was used for collecting the intensity data, indexing, and determination of lattice parameters, SAINT [29] was used for integration of the intensity of reflections and scaling, SADABS [30] was used for absorption correction, and SHELXTL [31] was used for space group and structure determination and least-squares refinements against *F*². Crystal and refinement data are summarized in Table 3.

The structures were solved by direct methods to locate the heavy atoms, followed by difference maps for the light, non-hydrogen atoms. The hydrogens were placed in calculated positions. The data for complex **9** is poor, and refinement was done at 2θ (max) = 45°. The terminal SMe group is disordered, splitting into two sets of positions 70:30 occupancy ratio. There are also solvent molecules present as space-filling solvent in complexes; viz. **2B** · 2MeCN and **9** · 2CH₂Cl₂.

Acknowledgements

We thank the National University of Singapore for Research Grant No. R143-000-209-112 to L.Y.G., research graduate scholarship to R.Y.C.S. and Dr. L.L. Koh and Ms. G.K. Tan for technical assistance.

Appendix A. Supplementary material

CCDC 633514, 633515, 633516 and 633517 contain the supplementary crystallographic data for **1B**, **2B**, **9** and **10**. These data can be obtained free of charge via <http://www.ccdc.cam.ac.uk/conts/retrieving.html>, or from the Cambridge Crystallographic Data Centre, 12 Union Road, Cambridge CB2 1EZ, UK; fax: (+44) 1223-336-033; or e-mail: deposit@ccdc.cam.ac.uk. Supplementary data associated with this article can be found, in the online version, at [doi:10.1016/j.jorganchem.2007.03.018](https://doi.org/10.1016/j.jorganchem.2007.03.018).

References

- [1] (a) P. Huston, J.H. Aspengon, A. Bakac, J. Am. Chem. Soc. 114 (1992) 9510; (b) M.T. Green, J. Am. Chem. Soc. 121 (1999) 7939; (c) J. Stubbe, D.G. Nocera, C.S. Yee, C.Y. Chang, Chem. Rev. 103 (2003) 2167; (d) M. Bennati, J.H. Robblee, V. Mugnaini, J. Stubbe, J.H. Freed, P. Borbat, J. Am. Chem. Soc. 127 (2005) 15014; (e) P. Wardman, Z.B. Alfassi (Eds.), S-Centered Radicals, Wiley, Chichester, 1999, pp. 289–309 (Chapter 10).
- [2] (a) D.T. Sawyer, G.S. Srivatsa, M.E. Bodinit, W.P. Schaefer, R.M. Wing, J. Am. Chem. Soc. 108 (1986) 936; (b) M. Kumar, R.O. Day, G.J. Colpas, M.J. Maroney, J. Am. Chem. Soc. 111 (1989) 5974; (c) K. Ray, T. Weyhermüller, A. Goossens, M.W.J. Crajé, K. Wieghardt, Inorg. Chem. 42 (2003) 4082; (d) C.A. Grapperhaus, S. Poturovic, Inorg. Chem. 43 (2004) 3292; (e) J.E. McDonough, J.J. Weir, K. Sukcharoenphon, C.D. Hoff, O.P. Kryatova, E.V. Rybak-Akimova, B.L. Scott, G.J. Kubas, A. Mendiratta, C.C. Cummins, J. Am. Chem. Soc. 128 (2006) 10295.
- [3] (a) M. Woods, J. Karbwang, J.C. Sullivan, E. Deutsch, Inorg. Chem. 15 (1976) 1678; (b) P.M. Treichel, L.D. Rosenhein, Inorg. Chem. 23 (1984) 4018, and references therein.
- [4] J. Springs, C.P. Janzen, M.Y. Darensbourg, J.C. Calabrese, P.J. Krusic, J.-N. Verpeaux, C. Amatore, J. Am. Chem. Soc. 112 (1990) 5789.
- [5] A.C. Lizano, M.G. Munchhof, E.K. Haub, M.E. Noble, J. Am. Chem. Soc. 113 (1991) 9204.
- [6] C.-H. Hsieh, I.-J. Hsu, C.-M. Lee, S.-C. Ke, T.-Y. Wang, G.-H. Lee, Y. Wang, J.-M. Chen, J.-F. Lee, W.-F. Liaw, Inorg. Chem. 42 (2003) 3925.
- [7] S. Kimura, B. Eckhard, E. Bothe, T. Weyhermüller, K. Wieghardt, J. Am. Chem. Soc. 123 (2001) 6025, and references cited therein.
- [8] (a) P.M. Treichel, M.S. Schmidt, R.A. Crane, Inorg. Chem. 30 (1991) 379; (b) B. Albela, E. Bothe, O. Brosch, K. Mochizuki, T. Weyhermüller, K. Wieghardt, Inorg. Chem. 38 (1999) 5131.
- [9] S. Poturovic, M.S. Mashuta, C.A. Grapperhaus, Angew. Chem. Int. Ed. 44 (2005) 1883.
- [10] R.Y.C. Shin, M.E. Teo, W.K. Leong, J.J. Vittal, J.H.K. Yip, L.Y. Goh, R.W. Webster, Organometallics 24 (2005) 1483.
- [11] L.Y. Goh, M.E. Teo, S.B. Khoo, W.K. Leong, J.J. Vittal, J. Organomet. Chem. 664 (2002) 161.
- [12] (a) C. Walling, W. Helmreich, J. Am. Chem. Soc. 81 (1959) 1144; (b) C. Chatgililoglu, M.P. Bertrand, C. Ferreri, Z.B. Alfassi (Eds.), S-Centered Radicals, Wiley, Chichester, 1999, pp. 311–354 (Chapter 11).
- [13] K.-D. Asmus, M. Bonifaèia, Z.B. Alfassi (Eds.), S-Centered Radicals, Wiley, Chichester, 1999, pp. 141–191 (Chapter 5), and references therein.
- [14] L. Pauling (Ed.), The Nature of the Chemical Bond, third ed., Cornell University Press, Oxford, 1960, p. 224 (Chapter 7).
- [15] B. Meyer, Chem. Rev. 76 (1976) 367, and references cited therein.
- [16] C.G. Kuehn, H. Taube, J. Am. Chem. Soc. 98 (1976) 689.
- [17] (a) J. Amarasekera, T.B. Rauchfuss, S.R. Wilson, Inorg. Chem. 28 (1989) 3875; (b) J. Amarasekera, T.B. Rauchfuss, S.R. Wilson, Inorg. Chem. 26 (1987) 3328.
- [18] D. Sellmann, P. Lechner, F. Knoch, M. Moll, J. Am. Chem. Soc. 114 (1992) 922.
- [19] (a) K. Matsumoto, T. Matsumoto, M. Kawano, H. Ohnuki, Y. Shichi, T. Nishide, T. Sato, J. Am. Chem. Soc. 118 (1996) 3597; (b) K. Matsumoto, H. Sugiyama, Acc. Chem. Res. 35 (2002) 915.
- [20] R.C. Elder, M. Trkula, Inorg. Chem. 16 (1977) 1048.
- [21] S. Kim, E.S. Otterbein, R.P. Rava, S.S. Isied, J. San Filippo Jr., J.V. Wasczyk, J. Am. Chem. Soc. 105 (1983) 336.

- [22] (a) R.Y.C. Shin, M.A. Bennett, L.Y. Goh, W. Chen, D.C.R. Hockless, W.K. Leong, K. Mashima, A.C. Willis, *Inorg. Chem.* 42 (2003) 95;
(b) R.Y.C. Shin, G.K. Tan, L.L. Koh, L.Y. Goh, *Organometallics* 23 (2004) 6293.
- [23] M.C. Thompson, D.H. Busch, *J. Am. Chem. Soc.* 86 (1964) 3651.
- [24] D. Sellmann, L. Zapf, *J. Organomet. Chem.* 289 (1985) 57.
- [25] D.C. Goodman, J.H. Reibenspies, N. Goswami, S. Jurisson, M.Y. Darensbourg, *J. Am. Chem. Soc.* 119 (1997) 4955, and references therein.
- [26] U. Koelle, J. Kossakowski, *Inorg. Synth.* 29 (1992) 225.
- [27] G. Rima, J. Satgé, M. Fatome, J.D. Laval, H. Sentenac-Roumanou, C. Lion, M. Lazraq, *Eur. J. Med. Chem.* 26 (1991) 291.
- [28] SMART Version 5.628, Bruker AXS Inc., Madison, Wisconsin, USA, 2001.
- [29] SAINT Version 6.22a, Bruker AXS Inc., Madison, Wisconsin, USA, 2001.
- [30] G.M. Sheldrick, *SADABS*, 1996.
- [31] SHELXTL Version 5.1, Bruker AXS Inc., Madison, Wisconsin, USA, 1997.